

Capacitive-coupled Grid-connected Inverter with Active Power Injection Ability

Wen-Chen Zhang,
Department of Electrical and Computer Engineering
University of Macau
Macao, SAR, P.R.China
Mb05510@umac.mo

Ning-Yi Dai, Man-Chung Wong, Chi-Kong Wong
Department of Electrical and Computer Engineering
University of Macau
Macao, SAR, P.R.China

Abstract—The capacitive-coupled grid-connected inverter (CGCI) system is proposed in this paper. It can reduce the active power from the grid by injecting active power from the PV generators into the grid. The reactive power and harmonic compensation ability of the CGCI leads to reduced root-mean-square (RMS) value of source current and thus reduced residential power loss. The proposed CGCI and conventional inductive-coupled grid-connected inverter (IGCI) are compared. Results indicate that CGCI can achieve the required power delivery with lower inverter voltage rating. The proposed CGCI is utilized to integrate a PV generation system to the grid. Besides, reactive power and harmonic compensation is achieved simultaneously when the active power is injected. A dynamic reactive power adjustment block is added to the control system of the CGCI, which can improve its performance when the required reactive power compensation exceeds its control capability. Simulation results are provided to verify the validity of the CGCI and its control system.

Keywords—capacitive-coupled grid-connected inverter, inductive-coupled grid-connected inverter, active power injection, reactive power and harmonic compensation

I. INTRODUCTION

The concept of Smart Home includes integrating different services within a home. It assures an economic, secure, comfortable and intelligent operation. This concept covers wide ranges of technologies, among which energy saving is the focus of this paper. Energy saving can be achieved by reducing the transmission loss of electricity power by means of reactive power and harmonic compensation. From the user's point of view, energy saving can be interpreted as reducing the electricity charge of the household by integration of renewable energy resource (RES) [1]. Hence, to achieve the target of energy saving with a cost-effective solution, a novel grid-connected inverter system is proposed in this paper, which offers active power delivery, reactive power compensation, and harmonic compensation.

A brief review in the areas of integration of RES as well as reactive power and harmonic compensation is given first. In addition to their active power delivery ability, the grid-connected PV (GCPV) system has been utilized to provide reactive power and harmonic compensation in recent development. Meanwhile, there is an increasing interest in the

PV inverters within domestic market, with requirements on higher efficiency, better reliability, and higher power quality of the output PV power. However, the inverter rating of the existing GCPV should be large enough for active, reactive power delivery and harmonic compensation. The existing approach connects the inverter to the grid by an inductor, so that dc-link voltage of the inverter is higher than utility level [2-6]. Hybrid power filter (HPF) provides reactive power and harmonic compensation with a reduced inverter rating. Particularly, the parallel HPF with a series combination of an inductor and a capacitor reduces the inverter voltage rating greatly, since the major fundamental voltage drops on the coupling capacitor. The research interests in the HPF systems both in home and abroad focus on the inverter control scheme and PWM modulation technique. No active power control ability has been studied in the existing HPF systems[7-9].

Therefore, to achieve the goals of active, reactive power delivery and harmonic compensation, a capacitive-coupled grid-connected inverter (CGCI) system is proposed in this paper. The inverter voltage can be reduced due to its capacitive coupling impedance, which results in reduced initial cost and running loss.

This paper is arranged as follows. In Section II, the comparison between conventional inductive-coupled grid-connected inverter (IGCI) system and the CGCI is carried out. Section III presents the characteristics of power flow in CGCI, which indicates the impact of the low inverter voltage rating on the power flow. Section IV describes the inverter control scheme. To fully utilize the RES devices, the active power injection is treated as the first priority when designing the control system. A reactive power adjustment block is included in this section. Finally, simulation verifications of the CGCI system are provided in Section V.

II. COMPARISON OF IGCI AND CGCI

A comparison between IGCI and CGCI is carried out in this section. The proposed grid-connected system is connected to the grid at the point of common coupling, where continuous reactive power compensation is required for the inductive loads. Hence, the load type is assumed to be inductive in this paper. In addition, the following discussions mainly focus on active and reactive power flow, thus the harmonic compensation is not considered in the comparison.

A. Model of IGCI and CGCI

Fig.1 shows the system configuration of IGCI and CGCI. In Fig.1, I_c indicates the inverter output current, and V_c indicates the voltage drop on the coupling impedance. The variable V_s represents the grid voltage, and V_{inv} , δ represent magnitude and phase angle of fundamental inverter output voltage, respectively. The P_{source} is the active power generated by the renewable energy source, and P_{inj} is positive when active power is injected into the grid from the inverter, Q_{inj} is positive when offering reactive power compensation for the inductive load.

The IGCI system is integrated into the grid by an inductor. The CGCI system is integrated by an inductor and a capacitor. An equivalent coupling capacitance C is introduced since coupling branch of the CGCI presents capacitive impedance at fundamental frequency. Thus, the amplitude and phase angle of the coupling impedance in these two systems can be written as in (1a)(1b)

$$Z_i = \omega L, \theta = 90^\circ; \quad (1a)$$

$$Z_c = 1/(\omega C), \theta = -90^\circ; \quad (1b)$$

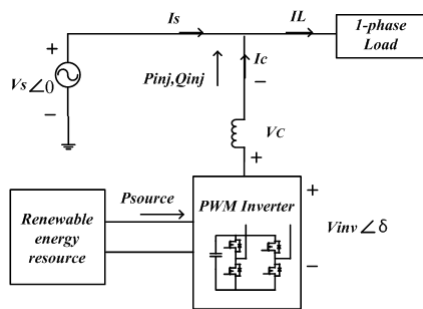
where ω represents the grid frequency, L indicates the coupling inductance of the IGCI, and C represents the equivalent coupling capacitance of the CGCI. The value of C can be estimated by the fundamental coupling impedance of the CGCI

$$X_{PF} = |\omega L_{PF} - 1/(\omega C_{PF})| = 1/(\omega C), \quad (2)$$

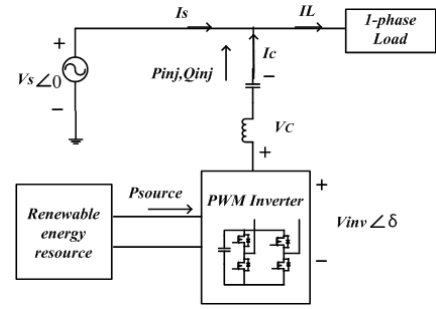
where L_{PF} and C_{PF} indicate the inductance and capacitance of the coupling branch in the CGCI system. Thus, equivalent capacitance is

$$C = C_{PF} / (1 - \omega^2 L_{PF} C_{PF}). \quad (3)$$

Fig.2 shows the equivalent circuits of IGCI and CGCI system, where load has been neglected so that the power flow and inverter output voltage in these two systems are focused on. The inverter is modelled as a fundamental ac voltage source. The harmonic components of the inverter output voltage that is caused by harmonic compensation are not involved in the models.



(a)IGCI system



(b)CGCI system

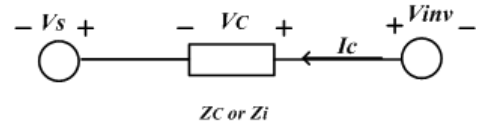


Figure 2. System configuration of IGCI and CGCI

B. Comparison of inverter output voltage

Assuming that the inverter output currents are the same in the IGCI and the CGCI, and can be written as

$$I_c = I_{c,d} - j I_{c,q}, \quad (4)$$

where $I_{c,d}$ is on the positive d-axis, indicating active power injection into the grid, while $I_{c,q}$ is on the negative q-axis, representing reactive power compensation for inductive load.

Fig.3 shows the corresponding current and voltage vector diagram. The voltage drop on the coupling impedance can be calculated by

$$\begin{aligned} V_{c,i} &= j \omega L * I_c \\ &= \omega L * I_{c,q} + j \omega L * I_{c,d}, \end{aligned} \quad (5a)$$

$$\begin{aligned} V_{c,c} &= -j I_c / (\omega C) \\ &= -I_{c,q} / (\omega C) - j I_{c,d} / (\omega C), \end{aligned} \quad (5b)$$

where $V_{c,i}$ and $V_{c,c}$ represent the voltage drop on the coupling impedance of IGCI and CGCI, respectively. According to the equivalent circuit model, the inverter output voltage is

$$V_{inv} = V_s + V_c. \quad (6)$$

Hence, the inverter output voltages in IGCI and CGCI are derived from (5)(6)

$$\begin{aligned} V_{inv,i} &= V_s + V_{c,i} \\ &= (V_s + \omega L * I_{c,q}) + j \omega L * I_{c,d}, \end{aligned} \quad (7a)$$

$$\begin{aligned} V_{inv,c} &= V_s + V_{c,c} \\ &= [V_s - I_{c,q} / (\omega C)] - j I_{c,d} / (\omega C), \end{aligned} \quad (7b)$$

where $V_{inv,i}$, $V_{inv,c}$ indicate the fundamental inverter output voltage in IGCI and CGCI, respectively. Based on (7), the inverter output voltage is shown in Fig.3, where following vectors are obtained

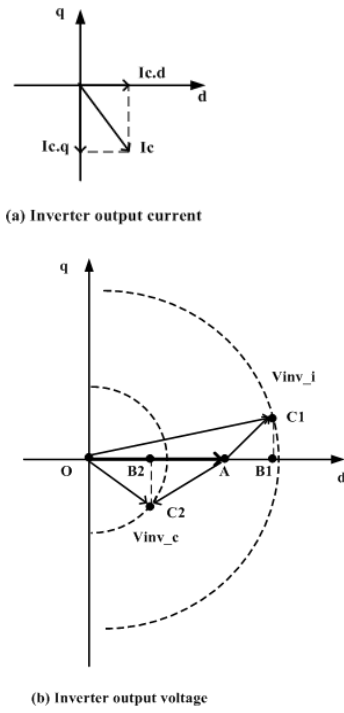


Figure 3. Inverter output voltage in IGCI and CGCI

$$\begin{aligned}
 \overline{OA} &= V_s, \overline{OC_1} = V_{inv,i}, \overline{OC_2} = V_{inv,c} \\
 \overline{AB_1} &= \omega L * I_{c,q}, \overline{AB_2} = -I_{c,q}/(\omega C) \\
 \overline{B_1C_1} &= j\omega L * I_{c,d}, \overline{B_2C_2} = -jI_{c,d}/(\omega C)
 \end{aligned} \quad (8)$$

Fig.3 shows that in order to provide active power injection and reactive power compensation for inductive load, the inverter output voltage in the IGCI should be higher than grid level, while its counterpart in the CGCI can be lower than the grid voltage. The low inverter voltage in the CGCI allows the adoption of low-voltage devices, which lead to reduced initial cost and running loss as well as less EMI. For a 220V ac system, the 400V MOSFETs can be adopted. Moreover, the reduced inverter voltage rating leads to reduced power rating of the inverter system [10].

III. CHARACTERISTICS OF POWER FLOW IN CGCI

The detailed power flow characteristics of the CGCI are studied in this section.

A. Power flow capacity of the CGCI system

According to power flow analyses, power flow between the CGCI and the grid are written as [11]

$$\begin{aligned}
 P_{inj} &= (V_s V_{inv} * \cos\delta / Z - V_s^2 / Z) * \cos\theta \\
 &\quad + V_s V_{inv} * \sin\delta * \sin\theta / Z,
 \end{aligned} \quad (9a)$$

$$\begin{aligned}
 Q_{inj} &= (V_s V_{inv} * \cos\delta / Z - V_s^2 / Z) * \sin\theta \\
 &\quad - V_s V_{inv} * \sin\delta * \cos\theta / Z,
 \end{aligned} \quad (9b)$$

where θ is the phase angle of the coupling impedance in the CGCI, which is -90° , and δ is the phase angle between the grid voltage and the inverter output voltage.

To neglect the influence of the coupling impedance on the power flow capacity, power base is defined as

$$S_{base_c} = V_s^2 \omega C. \quad (10)$$

As a result, the power flow in per unit form are given as

$$P_{inj} / S_{base_c} = -V_{inv,c} / V_s * \sin\delta \quad (11a)$$

$$Q_{inj} / S_{base_c} = -V_{inv,c} / V_s * \cos\delta + 1 \quad (11b)$$

Fig.4 shows the power flow in CGCI based on the per unit expressions. For a fixed voltage rating, δ can vary between $-\pi$ to π . Since the active power injection in (11a) is odd symmetrical, and reactive power in (11b) is even symmetrical, only the range of $-\pi$ to 0 is shown here. Within this range, active power is injected to the grid by the CGCI. Different curves represent different inverter voltage rating available in the CGCI. All the voltage rating in Fig.4 are lower than the grid voltage. It is clear that the CGCI can inject active power and offer reactive power compensation for inductive loads when the voltage rating is lower than grid voltage. However, Fig.4 shows that for a specified inverter voltage, the active power flow varies within a narrower range, compared to the range of corresponding reactive power flow. This is a major feature which should be considered in system design.

One case study is provided here. Suppose that CGCI is designed for residential application where the average active power consumption is about 2.5kW, and the average reactive power consumption is about 1200 Var [16]. Then the nominal reactive power compensation capacity is designed to be around one thousand Var. The equivalent capacitance C can be estimated by the average reactive power compensation requirement. Based on the characteristics of CGCI, the nominal active power flow should be smaller than the reactive power capacity. Moreover, to avoid the reverse power flow mode, which causes problems of voltage surge at terminal point and overloading of distribution transformer [13,14], the nominal active power flow should be smaller than load power at point of common coupling (PCC). Based

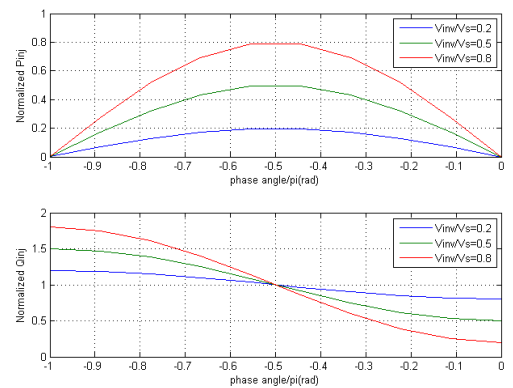


Figure 4. Power flow in CGCI

on the fact that the rating of most PV modules for residential users range from 90W to 500W [12], the nominal active power flow capacity of the CGCI can be chosen at about several hundred watts, which is much smaller than the average load power. The required power flow capacity locates inside the controllable range of the CGCI.

With the selected power delivery capacity and equivalent capacitance, the operation range of dc-link voltage can be estimated, which facilitates the choice of low-voltage devices.

B. Compensation range

For a selected dc-link voltage, the maximum allowable inverter output voltage is determined accordingly, thus imposing boundaries to the available power flow. According to inverter output current in Fig.3(a), Fig.5 shows the inverter output voltage in the CGCI, where red circle indicates the inverter voltage rating. The inverter can work at any point inside the circle. The maximum allowable inverter output voltage results in the reactive power compensation range at a specified active power injection level. Moreover, a larger active power injection corresponds to a narrower compensation range. In other words, the active power injection capacity of the CGCI system depends on the corresponding reactive power injection and the dc-link voltage.

Therefore, to guarantee the first priority of active power injection, and to ensure low inverter voltage rating, reactive power injection should be located within the compensation range.

The calculation of the compensation range is introduced as follows. In single-phase system, the inverter output voltage is related to the dc-link voltage as follows

$$V_{dc} = \sqrt{2} V_{inv} / M \quad (12)$$

where M indicates the modulation index, and is estimated as unity, and V_{dc} represents the selected dc-link voltage.

Under a given dc-link voltage and active power injection level, the reactive power compensation reaches its boundary at point A and B. Thus the inverter output voltages at point A and point B are

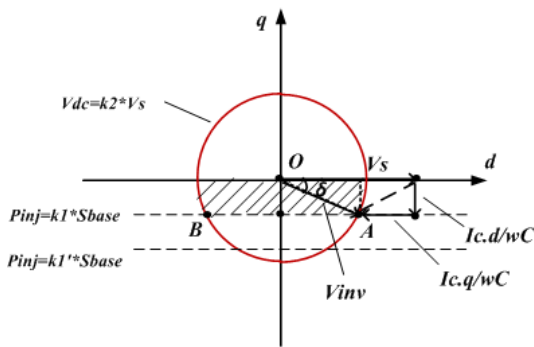


Figure 5. Inverter output voltage and compensation range in CGCI

$$V_{inv.A} = V_s * [(1 - Q_{inj.min} / S_{base_c})^2 + (P_{spec} / S_{base_c})^2]^{1/2}, \quad (13a)$$

$$V_{inv.B} = V_s * [(1 - Q_{inj.max} / S_{base_c})^2 + (P_{spec} / S_{base_c})^2]^{1/2}, \quad (13b)$$

where P_{spec} represents the specified active power injection, which is determined by the power generation of RES, and $Q_{inj.min}$, $Q_{inj.max}$ represent the lower and higher boundary of available reactive power injection.

Therefore, the compensation range can be determined based on the selected dc-link voltage and present active power generation of RES. Rewriting (12)(13), the compensation range is obtained

$$Q_{inj.adj1} = \{-[V_{dc}^2 / (2V_s^2) - (P_{inj} / S_{base_c})^2]^{1/2} + 1\} * S_{base_c}, \quad (14a)$$

$$Q_{inj.adj2} = \{[V_{dc}^2 / (2V_s^2) - (P_{inj} / S_{base_c})^2]^{1/2} + 1\} * S_{base_c}, \quad (14b)$$

where $Q_{inj.adj1}$, $Q_{inj.adj2}$ represent the lower and higher boundary of compensation range, P_{inj} represents the present active power injection.

During period of comprehensive active and reactive power injection, the load power may exceed the compensation range. The power variations lead to an over-large inverter output voltage and potential over-modulation mode of the inverter. The over-modulation deteriorates the performance of active power delivery and harmonic compensation. Therefore, it is necessary to carry out dynamic adjustment under wide load variation, so as to ensure the active power delivery and avoid over-modulation.

IV. OPERATION MODES AND CONTROL SCHEME OF CGCI SYSTEM

A. Operation modes of the CGCI system

The CGCI system is designed for active power delivery and reactive power compensation for the inductive load. The operation modes of the CGCI mainly include: (1) reactive power and harmonic compensation; (2) comprehensive active and reactive power flow, together with harmonic compensation.

When there is no active power injection requirement, the reactive power and harmonic compensation is obtained by direct current control scheme, which detects the average load reactive power and harmonic currents, and then calculates the reference compensation current by use of single-phase instantaneous reactive power theory (IRP). By PI current controller, the inverter output current can track its reference value with fast dynamic, thus achieving the required power delivery and compensation function.

When there is active power injection requirement, the CGCI operates in the mode of comprehensive active and reactive power delivery. The active power delivery is achieved by dc-link regulator, which ensures power balance of the overall inverter system, thus delivering the active power generation of RES into the utility grid. The reactive power and harmonic compensation are achieved simultaneously.

B. Inverter control system

The overall inverter control scheme is shown in Fig.6, which consists of dc-link regulation, reactive power adjustment, reference extraction, current controller, and PWM generator. The active power from RES is denoted as P_{source} . A negative PI regulator is used for dc-link voltage control. The output of the PI regulator, denoted as PI_out , is added to the active power P_{source} from RES, to form the dc component of active power injection reference $P_{inj_dc}^*$. Although the voltage control loop can work alone for generating the reference of active injecting current [5,6], the feedforward information P_{source} is added to accelerate the dynamic response [15]. Moreover, due to the capacitive coupling impedance, PI_out is also added to the reactive power reference, as investigated in [7,8]. The reactive power adjustment module restricts the dc component of reactive power reference within the compensation range. Since $P_{inj_dc}^*$ reflects the active power injection into the grid, it is employed as input to the reactive power adjustment module.

The compensation range can be determined by a look-up table, as shown in Table I. The P_{inj_max} represents the maximum active power injection according to system design, which is $1/3 * S_{base}$ in this paper, and the dc-link voltage is assumed as 0.6 times of grid voltage.

The harmonic compensation is also achieved in the control block. the ac components of load power, denoted as $p_{L,h}$, $q_{L,h}$, are incorporated in the reference injection power. The carrier wave PWM generator is employed for pulse generation, with a switching frequency of 10kHz.

V. SIMULATION RESULTS

In order to verify the functions of the CGCI, simulations have been carried out using PSCAD. The simulation circuit and the load model can be referred to Fig.7, where energy source (PV array) is modelled by a PWM rectifier. Table II shows the system parameters.

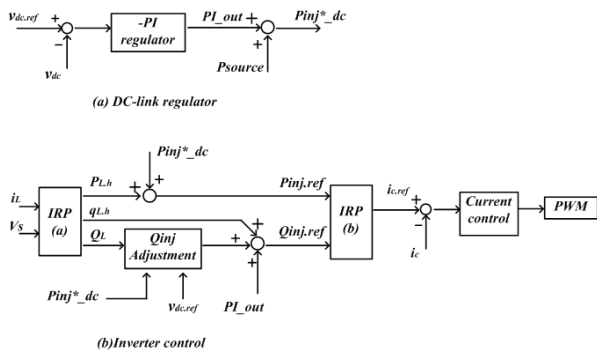


Figure 6. Control scheme of CGCI

TABLE I. REACTIVE POWER ADJUSTMENT

dc-link voltage	Active power injection	Compensation range
$V_{dc} = 0.6V_s$	$P_{inj1} = 1/9 * S_{base}$	$[0.5905, 1.4095] * S_{base}$
	$P_{inj2} = 2/9 * S_{base}$	$[0.6385, 1.3615] * S_{base}$
	$P_{inj,max} = 1/3 * S_{base}$	$[0.7374, 1.2626] * S_{base}$

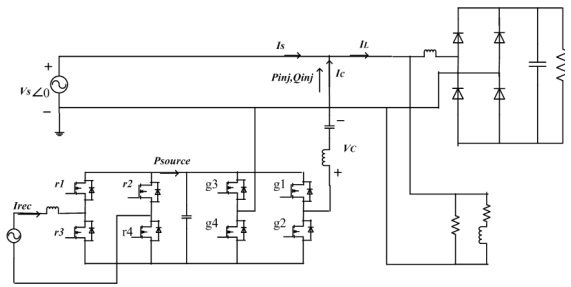


Figure 7. Simulation circuit of the CGCI

TABLE II. SYSTEM PARAMETERS

Grid voltage	220 V
Switching frequency	10 kHz
Filter inductor	3.5 mH
Filter capacitor	60 uF
Resonant frequency	347 Hz
Power base	912 VA
dc-link capacitor	2000 uF
dc-link voltage	130 V

Fig.8, Fig.9, Fig.10 show the simulation results, where V_s indicates grid voltage, I_s , I_{load} represent source current and load current, respectively, and V_{dc} , $V_{dc.ref}$ represent dc-link voltage and its reference value, respectively. Fig.8 shows the performance of the CGCI when only reactive power and harmonics of the load need to be compensated. Simulation results are listed in Table III, which show the feasibility of the CGCI.

Fig.9 presents the system performance when active power, reactive power and harmonics are injected to the grid by the CGCI. Before 1.0s, the active power can trace the power from RES and the reactive power can trace the load reactive power. Table IV gives the corresponding indexes at the load side and source side.

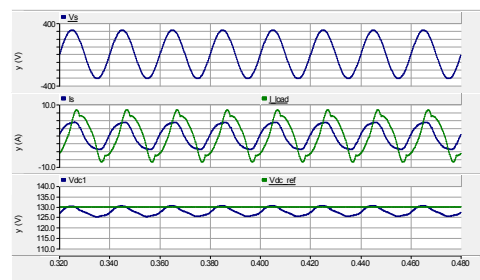
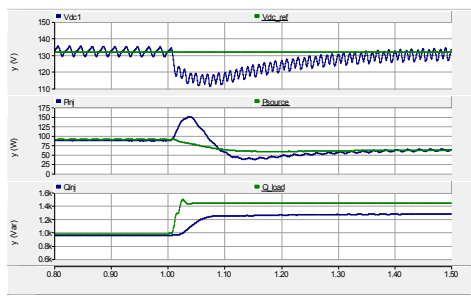


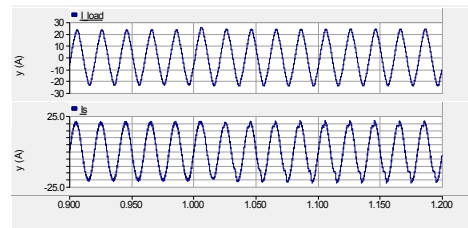
Figure 8. Performance of CGCI under no active power injection

TABLE III. PERFORMANCE OF CGCI UNDER NO ACTIVE POWER INJECTION (DC-LINK VOLTAGE: 130V, NORMAL LOAD)

	Power	Power factor	Current THD	RMS
Load	3248W, 977Var	0.957	5.34%	15.5A
Source side	3248W, 4Var	0.998	1.12%	14.8A

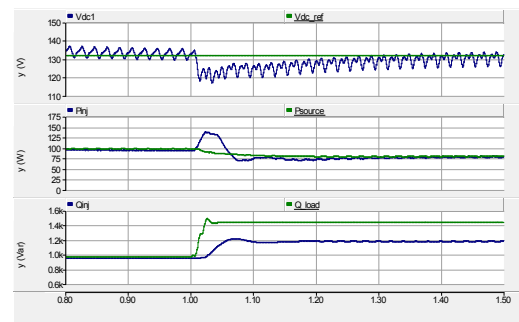


(a)DC-link voltage and power injection

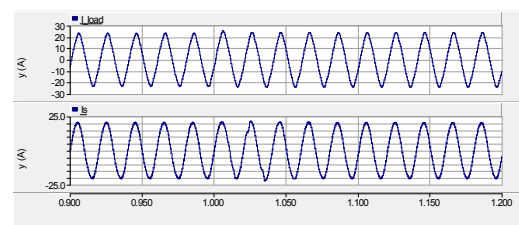


(b)Current waveform

Figure 9. Performance of CGCI without reactive power adjustment (heavy load)



(a)DC-link voltage and power injection



(b)Current waveform

Figure 10. Performance of CGCI with reactive power adjustment (heavy load)

TABLE IV. PERFORMANCE OF CGCI WITH ACTIVE POWER INJECTION (NORMAL LOAD)

	Power	Power factor	Current THD	RMS
Load before 1.0s	3248W, 977Var	0.957	5.34%	15.5A
Source side	3155W, 27Var	0.998	1.48%	14.3A

After 1.0s, the load reactive power increases to exceed the compensation range. Fig.9 presents the system performance without reactive power adjustment. Due to the insufficient dc-link voltage, duty-cycle saturation occurs, leading to distorted source current and slow stabilization of dc-link voltage. Moreover, the deteriorated dc-link voltage loop results in quite an amount of variation in active power injection. Fig.10 shows the system performance with reactive power adjustment. Due to the reactive power adjustment, duty-cycle saturation has been avoided. Thus, there is a faster transient response in the dc-link voltage, which results in consequently reduced variation in active power injection. Table V show the performance improvement due to the reactive power adjustment. In order to guarantee the required active power injection and to avoid over-modulation, the reactive power is partially compensated.

TABLE V. PERFORMANCE OF CGCI UNDER HEAVY LOAD

	Power	Power factor	Current THD	RMS
Load after 1.0s	3185W, 1440Var	0.915	4.40%	15.9A
Source side without adjustment	3122W, 168Var	0.996	11.3%	14.3 A
Source side with adjustment	3105W, 259Var	0.984	1.69%	14.2A

VI. CONCLUSIONS

The CGCI system is proposed in this paper, which is capable of offering comprehensive power delivery and harmonic compensation. Compared to traditional IGCI system, the CGCI system greatly reduces the inverter voltage rating, without deteriorating the ability of power delivery and harmonic compensation. The reactive power adjustment module is included in the inverter control scheme, aiming at ensuring the required amount of active power injection and low inverter output voltage when load power exceeds the compensation range. The feasibility of the CGCI system and effectiveness of reactive power adjustment have been verified by simulation results.

ACKNOWLEDGMENTS

The authors would like to thank the Research Committee of University of Macau for their financial support.

Reference

- [1] R Lutolf, "Smart Home Concept and the Integration of Energy Meters into a Home Based System", Metering apparatus and tariffs for electricity supply, 7th international conference, 1992, pp.277-278.
- [2] Torrey, et.al., " Inverter Topology for Utility Interactive Distributed Generation Units", US patent 10777258.
- [3] TSAI-FU WU, CHIH-LUNG SHEN, CHIEN-HSUAN CHANG, JENANG CHIU, " 1 phase 3W Grid-Connection PV Power Inverter with Partial Active Power Filter" , IEEE Transactions on Aerospace and Electronic System, VOL. 39, NO. 2 APRIL 2003, pp. 635-646.
- [4] S.Kim, Gwonjong Yoo, Jinsoo Song, " A bifunctional utility connected photovoltaic system with power correction and UPS facility" , 25th IEEE Photovoltaic specialists conference, 1996, pp. 1363-1368.
- [5] Frede Blaabjerg, Remus Teodorescu, Marco Liserre, and Adrian V. Timbus, " Overview of Control and Grid Synchronization for Distributed Power Generation Systems", IEEE Transactions on Industrial Electronics, VOL. 53, NO. 5, OCTOBER 2006, pp. 1398-1409.
- [6] Yaow-Ming Chen, Hsu-Chin Wu, Yung-Chu Chen, Kung-Yen Lee, and Shian-Shing Shyu, " The AC Line Current Regulation Strategy for the

- Grid-Connected PV System”, IEEE Transactions on Power Electronics, VOL. 25, NO. 1, JANUARY 2010, pp. 209-218.
- [7] Salem Rahmani, Abdelhamid Hamadi, Nassar Mendalek, ” A New Control Technique for Three-Phase Shunt Hybrid Power Filter” , IEEE Transactions on Industrial Electronics, VOL. 56, NO. 8, AUGUST 2009, pp. 2904-2915.
- [8] Hideaki Fujita and Hirohmi Akagi, ” A Practical Approach to Harmonic Compensation in Power Systems-Series Connection of Passive and Active Filters” , IEEE Transactions on Industrial Applications, VOL. 21, NO. 6, NOVEMBER/DECEMBER 1991, pp. 1020-1025.
- [9] Sunt Srianthumrong and Hirofumi Akagi, ” A Medium-Voltage Transformerless AC/DC Power Conversion System Consisting of a Diode Rectifier and a Shunt Hybrid Filter”, IEEE Transactions on Industrial Applications, VOL. 39, NO. 3, MAY/JUNE 2003, pp. 874-882.
- [10] Hirofumi Akagi, Fellow, IEEE, Sunt Srianthumrong, and Yasuhiro Tamai, “ Comparisons in Circuit Configuration and Filtering Performance between Hybrid and Pure Shunt Active Filters”, Industry Applications Conference, Page(s): 1195 - 1202 vol.2.
- [11] Josep M. Guerrero, Jose Matas, Luis Garcia de Vicuna, Miguel Castilla, and Jaume Miret, ” Wireless-Control Strategy for Parallel Operation of Distributed-Generation Inverters ” , IEEE Transactions on Industrial Electronics, VOL. 53, NO. 5, OCTOBER 2006, pp. 1461-1470.
- [12] Quan Li, and Peter Wolfs, ” A Review of the Single Phase Photovoltaic Module Integrated Converter Topologies with Three Different DC Link Configurations”, IEEE Transactions on Power Electronics, VOL. 23, NO. 3, MAY 2008, pp. 1320-1333.
- [13] Farid Katiraei, Julio Romero Aguero, ” Solar PV Integration Challenges”, IEEE Power and Energy Magazine, VOL.9, NO. 3, 2011, pp. 62-71.
- [14] B. Verhoeven et al., Utility Aspects of Grid Connected Photovoltaic Power Systems. International Energy Agency Photovoltaic Power Systems, IEA PVPS T5-01: 1998. [Online]. Available: www.iea-pvps.org.
- [15] Luigi Malesani, Leopoldo Rossetto, Paolo Tenti, Paolo Tomasin, ” AC/DC/AC PWM Converter with Reduced Energy Storage in the DC Link”, IEEE Transactions on Industrial Applications, VOL. 31, NO. 2, APRIL 1995, pp. 287-292.
- [16] Troy A. Nergaard, Jeremy F. Ferrell, Leonard G. Leslie, and Jih-Sheng Lai, ” Design Considerations for a 48 V Fuel Cell to Split Single Phase Inverter System with Ultracapacitor Energy Storage”, Power Electronics Specialist Conference, 2002, Vol.4 , Page(s): 2007 – 2012.